

Ag Nanowire Reinforced Highly Stretchable Conductive Fibers for Wearable Electronics

Seulah Lee, Sera Shin, Sanggeun Lee, Jungmok Seo, Jaehong Lee, Seungbae Son, Hyeon Jin Cho, Hassan Algadi, Saleh Al-Sayari, Dae Eun Kim, and Taeyoon Lee*

Stretchable conductive fibers have received significant attention due to their possibility of being utilized in wearable and foldable electronics. Here, highly stretchable conductive fiber composed of silver nanowires (AgNWs) and silver nanoparticles (AgNPs) embedded in a styrene-butadiene-styrene (SBS) elastomeric matrix is fabricated. An AgNW-embedded SBS fiber is fabricated by a simple wet spinning method. Then, the AgNPs are formed on both the surface and inner region of the AgNW-embedded fiber via repeated cycles of silver precursor absorption and reduction processes. The AgNW-embedded conductive fiber exhibits superior initial electrical conductivity ($\sigma_0 = 2450 \text{ S cm}^{-1}$) and elongation at break (900% strain) due to the high weight percentage of the conductive fillers and the use of a highly stretchable SBS elastomer matrix. During the stretching, the embedded AgNWs act as conducting bridges between AgNPs, resulting in the preservation of electrical conductivity under high strain (the rate of conductivity degradation, $\sigma/\sigma_0 = 4.4\%$ at 100% strain). The AgNW-embedded conductive fibers show the strain-sensing behavior with a broad range of applied tensile strain. The AgNW reinforced highly stretchable conductive fibers can be embedded into a smart glove for detecting sign language by integrating five composite fibers in the glove, which can successfully perceive human motions.

1. Introduction

Recently, stretchable electronics have been widely researched due to their potential applications from wearable devices to foldable electronics, including flexible displays, flexible energy devices, smart skins, and stretchable circuits.^[1–5] For realization of the stretchable devices, research on stretchable conductors is required to retain electrically and mechanically stable properties under deformation.^[6–10] Among this research, stretchable conductive fibers based on soft polymers have attracted the interest of numerous researchers since soft polymer-based fibers are inherently stretchable, cost-efficient, and can even be weaved into various types of fabrics. Several studies on stretchable conductive fibers have been reported using various methods such as a polyurethane and poly(3,4-ethylenedioxythiophene):poly(styrene-sulfonate) (PEDOT:PSS) mixed conductive fiber using wet spinning method,^[11] poly(styrene- β -isobutylene- β -styrene) and poly(3-hexylthiophene) composite fiber by chemical doping,^[12] and

liquid-exfoliated graphene-infused natural rubber composites using dip coating method.^[13]

However, it is very difficult to simultaneously satisfy both high conductivity and high mechanical stretchability at the same time since these two indispensable factors seem to be mutually exclusive. To achieve high conductivity under a strained state, some researchers used highly stretchable elastomeric polymer fibers consisting of liquid metal or highly conductive fillers. Zhu et al. described the fabrication process and characterizations of fibers consisting of a liquid metal alloy (eutectic gallium indium) existing in the core of stretchable hollow fibers composed of a triblock copolymer resin.^[14] The obtained fiber showed ultra-stretchable and metallic electrical conductivity, however, they have some limitations: the core of the fiber can be collapsed and easily damaged under concentrated pressure, large strains, or from cutting. Ma et al. reported silver (Ag) particles decorated multiwalled carbon nanotubes (*n*Ag-MWNTs) in a poly(vinylidene fluoride-co-hexafluoropropylene) matrix (PVDF-HFP) to fabricate highly conductive stretchable fibers.^[15] Although the initial conductivity (σ_0) was $17\,460 \text{ S cm}^{-1}$, the maximum strain at rupture was only $\approx 60\%$

S. Lee, S. Shin, S. Lee, Dr. J. Seo, J. Lee, H. Algadi, Prof. T. Lee

Nanobio Device Laboratory
School of Electrical and Electronic Engineering
Yonsei University
50 Yonsei-ro, Seodaemun-Gu, Seoul
120-749, Republic of Korea
E-mail: taeyoon.lee@yonsei.ac.kr

S. Son, Prof. D. E. Kim
Biological Cybernetics Laboratory
School of Electrical and Electronic Engineering
Yonsei University
50 Yonsei-ro, Seodaemun-gu, Seoul 120-749, Republic of Korea

H. J. Cho
Krieger School of Arts & Sciences
Advanced Academic Programs
Johns Hopkins University
1717 Massachusetts Ave, NW Washington, DC 20036, USA

Prof. S. Al-Sayari
Promising Center for Sensors and Electronic Devices
Najran University
1988, Najran 11001, Saudi Arabia

DOI: 10.1002/adfm.201500628



and the rate of conductivity degradation (σ/σ_0) was 0.083% at 100% strain. Therefore, studies on the highly conductive stretchable fibers which maintain their electrical properties under high mechanical strain should be performed.

In this paper, we fabricated highly stretchable conductive fibers composed of silver nanowires (AgNWs), silver nanoparticles (AgNPs), and poly(styrene-*block*-butadiene-*block*-styrene, SBS) polymer. The AgNW-mixed SBS fiber was fabricated by a facile wet spinning method using an AgNW-dispersed SBS solution dope. An AgNP precursor was adsorbed in wet-spun AgNW-mixed SBS fiber, and then converted into AgNPs directly inside and outermost surface of the fiber. The highest conductivity and maximum elongation at break obtained by the AgNW–AgNP embedded composite fibers were 2450 S cm^{-1} and 900%, respectively. The composite fiber did not lose its electrical connections until 220% stretching and preserved the conductivity due to the networks of the AgNPs and AgNWs inside the SBS fiber. We confirmed that the AgNWs were aligned along the applied uniaxial strain and they can bridge the

disconnected networks of AgNPs. To demonstrate the capability of our fiber, we integrated the composite fibers into a wearable glove for detecting sign language, and successfully recognized the motions of the human hand by its strain-sensing behavior.

2. Results and Discussion

Figure 1a illustrates the procedure for fabricating the highly stretchable AgNW–AgNP embedded SBS composite fiber. The procedure involves two main steps: a wet spinning method to synthesize AgNW-mixed SBS fiber, and Ag precursor adsorption and reduction to fabricate the conductive fiber. An SBS polymer fiber mixed with AgNWs was produced by a solvent/nonsolvent wet spinning method. The average diameter and length of the AgNWs synthesized by a modified CuCl_2 -mediated polyol process^[16,17] were 104.6 nm and 20.4 μm , respectively (Figure S1, Supporting Information). The synthesized AgNWs were uniformly mixed with the SBS polymer solution, of which a

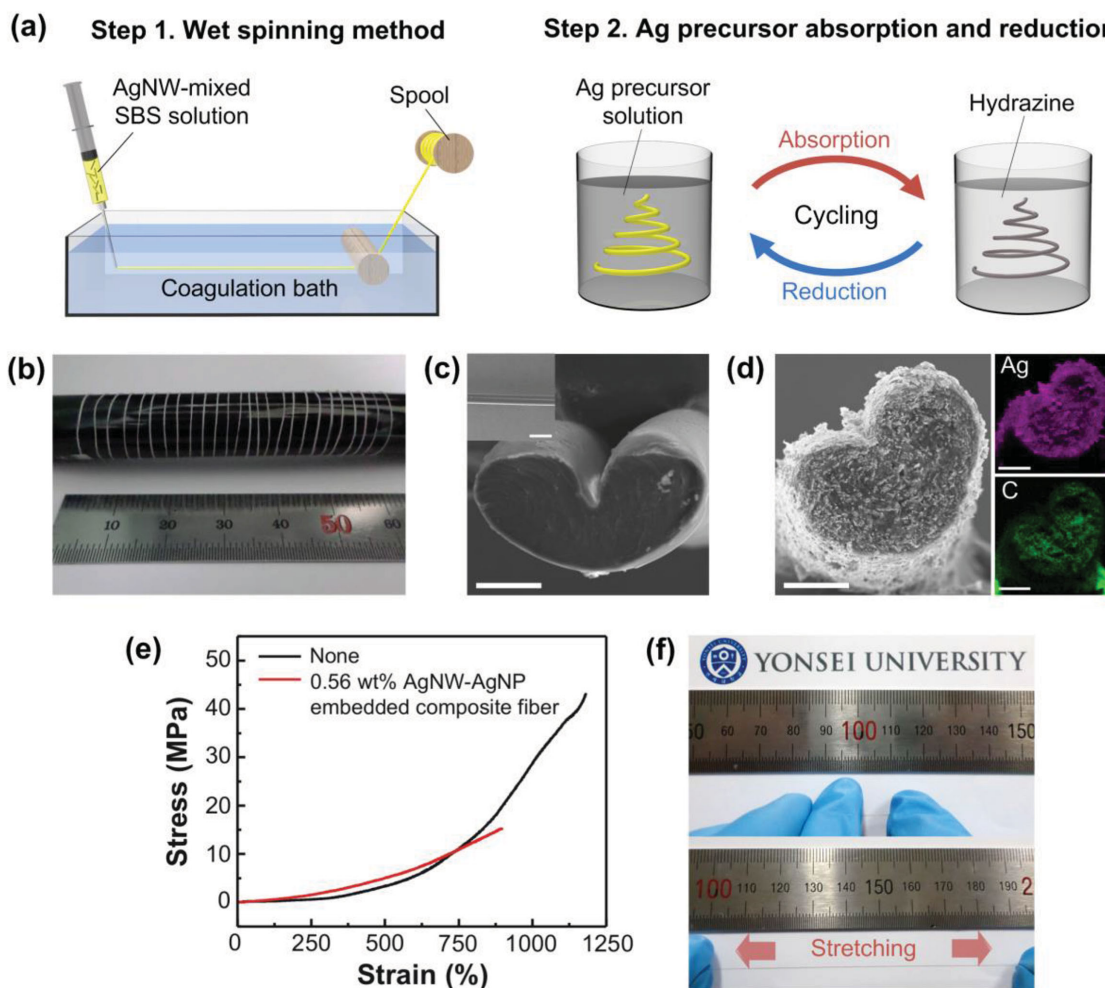


Figure 1. a) Schematic illustration of the fabrication process for the highly stretchable conductive fiber. b) Photograph of 0.56 wt% AgNW-mixed SBS fiber collected on a long cylindrical shaped spool. c) Cross-sectional SEM image of 0.56 wt% AgNW-mixed SBS without AgNP. Scale bar: 100 μm . (The inset shows the plan-view of as-wet-spun SBS fiber. Scale bar: 500 μm .) d) Cross-sectional SEM image and EDS mapping images of Ag, and C obtained from the 0.56 wt% AgNW–AgNP embedded composite fiber. Scale bar: 100 μm . e) Stress–strain curves for tensile tests on SBS fiber and 0.56 wt% AgNW–AgNP embedded composite fiber. f) Optical images of pre- and 900%-strained composite fiber.

solvent is a mixture of *N,N*-dimethylformamide (DMF) and tetrahydrofuran (THF), and then the AgNW-mixed SBS solution was injected into the polyvinyl alcohol (PVA) coagulation liquid. The precipitation of the SBS polymer occurred immediately when the SBS solution was injected into the PVA coagulation liquid. Prior to the establishment of this solvent/nonsolvent wet spinning method system, we investigated suitable solvents and coagulation liquids by examining their Hildebrand and Hansen solubility parameters, which can be used as an indication of solubility between materials.^[18] When the values of the Hildebrand and Hansen parameters of the materials are similar, they can be miscible. In our system, the PVA coagulation liquid, DMF/THF solvent mixture, and SBS polymer used in the wet spinning method satisfy this relationship. The calculated solubility parameter of the DMF/THF (wt/wt = 3:1) mixture is 20.1 MPa^{1/2}.^[19] The solubility parameter of the SBS polymer calculated in terms of the weight ratio of styrene/butadiene being 70/30 is 17.7 MPa^{1/2}.^[20] Since the solubility parameter of the SBS polymer is similar to that of the DMF/THF solvent, SBS can be soluble in the mixture of the DMF/THF solvent. However, as a result of the solubility parameter of PVA ranged from 27.6 to 28.4 being different from that of SBS and the DMF/THF solvent mixture, it could be used as the nonsolvent material for producing the SBS fiber via the wet spinning method.^[21] As shown in Figure 1b, a 100 cm long example of wet-spun 0.56 wt% AgNW-mixed SBS polymer fiber could be successfully obtained and collected on a long cylindrical-shaped spool. The fabrication speed of the polymer fiber was 1.14 cm s⁻¹ and it could be enhanced by increasing the injection rate of the polymer solution and rotation speed of spool.

Figure 1c shows a typical cross-sectional field emission scanning electron microscope (FE-SEM) image of the 0.56 wt% AgNW-mixed SBS fiber. The cross-sectional morphology of the 0.56 wt% AgNW-mixed SBS fiber was noncircular and had a bean-shaped structure, of which the width ranged from 150 to 200 μm (the inset of Figure 1c). This interesting shape of the fiber can be influenced by the temperature and concentration of the coagulation liquid which can affect the coagulation rate of the fiber during the wet spinning method.^[22,23] When the temperature and the concentration of coagulation liquid are low, the coagulation rate of the fiber is also low because the outward diffusion of the solvent of polymer can be more dominant than the inward diffusion of the coagulation liquid. Since the rate of the outward diffusion of the fiber is higher than that of the inward diffusion, an internal osmotic pressure can occur, which might lead to the bean-shaped structure. Furthermore, a wet-spun fiber synthesized in the bath with a low temperature can have a large amount of long-chain molecules because the molecular chains can be aligned more effectively along the spinning direction. Thus, the bean-shaped fiber fabricated by our wet spinning system can exhibit superior mechanical stretchability.

Figure 1d represents a cross-sectional SEM image of the 0.56 wt% AgNW–AgNP embedded SBS fiber, and corresponding energy dispersive spectrometer (EDS) mapping images of the fiber. The corresponding EDS spectrum with the peak of Ag atom is shown in Figure S2 (Supporting Information). The 0.56 wt% AgNW–AgNP embedded SBS fiber was fabricated by sequential processes of Ag precursor absorption

and hydrazine reduction.^[5] Since the trifluoroacetate anions (CF₃COO⁻) of the AgCF₃COO precursor can interact with the hydroxyl groups (–OH) of the ethanol solvent, a large amount of Ag precursor solution is absorbed into the fiber in a short amount of time. When the swollen fiber containing the Ag precursor solution was dipped in the hydrazine solution, the Ag precursor was reduced and changed into AgNPs inside and outermost surface of the fiber. Even after three cycles of the 0.56 wt% AgNW–AgNP, the bean-shaped structure of the fiber was maintained. As shown in the EDS mapping image of an Ag atom in Figure 1d, the formed AgNPs uniformly and fully existed not only on the surface of the fiber, but also inside the fiber in high density. The densely generated AgNPs at both inside and outermost surface of the fiber were connected with each other and formed the highly conducting path. In Figure 1d, as expected, existence of carbon atoms was observed at the whole cross-sectional area of the fiber originating from the SBS polymer matrix. We also investigated the contribution of the AgNPs on the surface of the fiber to electrical performance by scraping off the AgNPs from the surface using 3M tape (Figure S3, Supporting Information). The conductivity of the surface-scraped and 0.56 wt% AgNW–AgNP embedded composite fiber was decreased to 603 S cm⁻¹ compared to that of the nonscraped composite fiber. However, the scraped composite fiber preserved its electrical property up to 190% strain which is similar to that of the 0.56 wt% AgNW–AgNP embedded fiber. Furthermore, we compared our composite fiber with other conductive fibers fabricated by the electroless deposition of the metal on polymer because the metal deposited by this method is only existed on the surface of polymer fiber. Many of them reported the high-strength conductive fibers using the electroless-deposited metal on high-strength polymer fiber,^[24,25] and submicrometer-sized metal tubes using polymer fibers as a template.^[26,27] However, we assume that the electroless deposition method would not be applicable to the stretchable conductive fiber because the metal layer on the surface of fiber is physically and easily broken under mechanical deformation. Since the electrical network is only existed on the surface of fiber, the fracture of the metal layer on the surface can cause the loss of the electrical conducting path of the conductive fiber. Thus, AgNPs inside the composite fiber would mainly contribute the preservation of electrical property under strain.

To observe the mechanical properties of the fibers, we measured the strain–stress curves of the wet-spun SBS and the 0.56 wt% AgNW–AgNP embedded SBS composite fibers (Figure 1e). The value of the elongation at break of composite fiber (900%) was decreased compared with that of as-wet-spun fiber (1182%). Otherwise, the yield strength of the composite fiber was 2.8 MPa, which was larger than 2.4 MPa for the as-wet-spun fiber. This can be attributed to the increase in the stiffness of the composite fiber, which is caused by adding rigid fillers of AgNWs and AgNPs into the SBS elastomeric matrix. Furthermore, as the elongation at break of the composite fiber is still a considerably high value, although it decreased slightly, we can describe the AgNW–AgNP embedded fiber as having a highly stretchable characteristic. Figure 1f is a photograph of the composite fiber before and after stretching, and shows the excellent mechanical stretchability of the fiber.

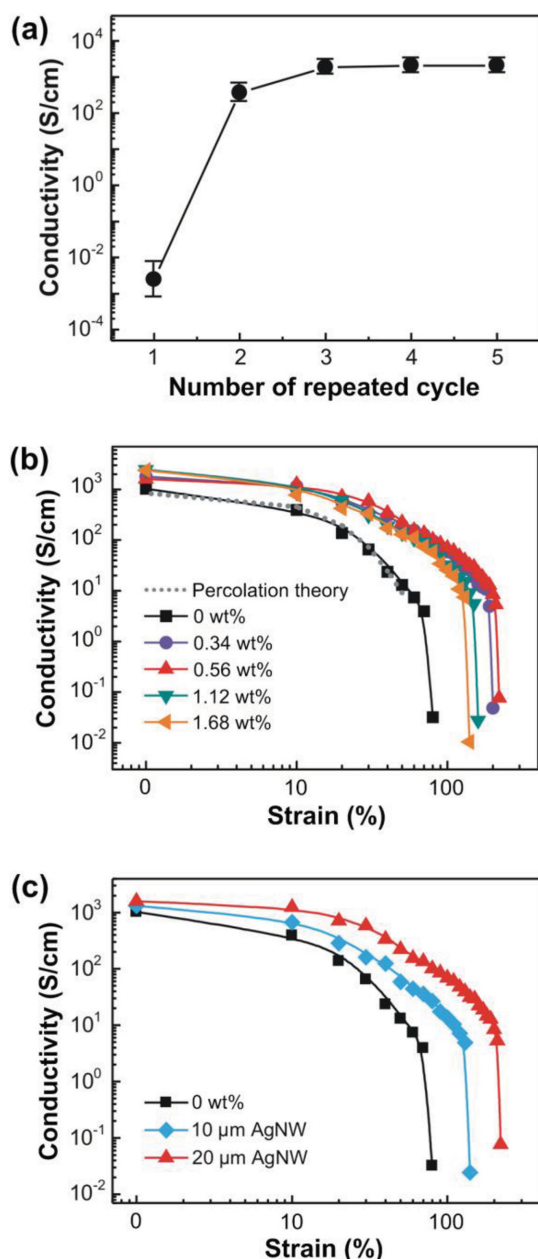


Figure 2. Electrical properties of the fabricated fibers depending on the applied uniaxial strain. a) Initial conductivities of fibers depending on the number of repeated processes for Ag precursor absorption and hydrazine reduction. b) Changes in conductivity of fibers fabricated by different concentrations of AgNWs with increasing strain. c) Changes in conductivity of the composite fiber fabricated by different length of AgNWs with increasing strain.

To observe the electrical properties of the conductive fibers by varying the number of the repeated cycles of the Ag absorption and reduction (step 2 in Figure 1a), the initial conductivities of the AgNP-embedded SBS conductive fibers without AgNWs were measured as a function of the number of the repeated cycles (Figure 2a). The initial conductivity was gradually increased according to the number of repeated cycles, and then saturated when the conductive fiber was treated over three

times of repeated cycles. This can be explained by the increase in the concentration of the AgNPs formed by the Ag precursor absorption and reduction in the SBS fiber depending on the number of repeated cycles, which were confirmed by thermogravimetric analysis (TGA) (Figure S4, Supporting Information). The samples with three times of Ag precursor absorption and reduction processes were used in the following analysis.

Figure 2b shows the curves of the electrical conductivities of the AgNW–AgNP embedded composite fiber under uniaxial strain by varying the concentration of the AgNWs (0, 0.34, 0.56, 1.12, and 1.68 wt%). The initial conductivities of the AgNW–AgNP composite fibers increased as the weight percentage of the AgNWs increased. The highest initial conductivity obtained from the 1.68 wt% AgNW–AgNP embedded composite fiber was 2450 S cm⁻¹. Without the AgNWs, the experimental conductivity data (black square symbol) of the AgNP-embedded SBS fiber corresponded to the theoretically calculated conductivity values (gray dashed line), which were obtained from the 3D percolation theory^[28] and the interparticle distance model.^[29] (See the Supporting Information for details.) A disconnection of the AgNPs in the AgNP-embedded SBS fiber without AgNWs occurred at a 70% strain. In contrast, the maximum strains at which the composite fiber did not lose its electrical conductivity significantly increased with values of 80%, 200%, 220%, 160%, and 140% corresponding to the AgNW concentrations of 0, 0.34, 0.56, 1.12, and 1.68 wt%, respectively. All of the AgNW–AgNP embedded composite fibers showed larger maximum strains compared to that of the AgNP-embedded fiber without AgNWs. Interestingly, the electrical property under strain is not linearly enhanced according to the AgNW concentrations, and the 0.56 wt% AgNW-mixed composite fiber shows the best performance in terms of both stretchability (220% of maximum strain) and conductivity ($\sigma/\sigma_0 = 4.4\%$ at 100% strain). This can be attributed to the fact that when too many AgNWs were mixed in the SBS solution for the wet spinning method (>0.56 wt%), AgNWs may be aggregated with each other due to the van der Waals interactions and affect the dispersion of AgNWs in highly viscous SBS polymer solution.^[30] The aggregated AgNWs would hinder the charge transfer between conductive fillers (AgNWs and AgNPs), thereby lowering the electrical conductivity of the composite material. In order to observe the effects of the length of the AgNWs, we investigated the conductivity–strain curves of the composite fibers mixed with no AgNWs, and a 10 μm length and 20 μm length of AgNWs at a concentration of 0.56 wt%. When the length of the AgNWs was increased, the conductivity and maximum strain were enhanced. This can be explained by the percolation threshold, which is defined as a critical value of the occupation probability for the formation of long-range connectivity in the composite matrix contained with conductive fillers. The percolation threshold will decrease according to the increase in the length of the AgNWs in the composite fiber resulting in an improvement in the electrical properties.^[30]

The increment of the stretchability of the AgNW-embedded highly stretchable conductive fibers could be explained by the AgNW-induced electrical connection of the broken electrical networks between AgNPs under mechanical deformation. Figure 3a illustrates the longitudinal regions inside the conductive fibers with/without AgNWs before (left) and after (right)

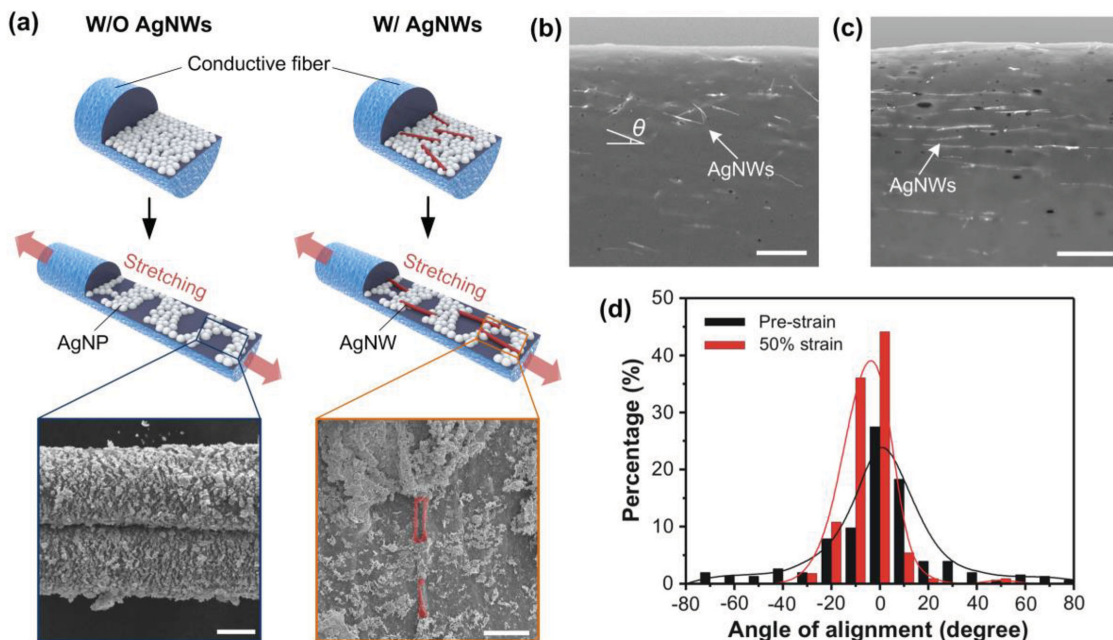


Figure 3. a) Schematic illustration of changes in AgNWs and AgNPs in the composite fiber. (Left navy-lined box: SEM image of the AgNP-mixed SBS fiber without AgNWs at 50% strain. Scale bar: 30 μm . Right red-lined box: SEM image of the 0.56 wt% AgNW–AgNP embedded SBS fiber at 50% strain. Scale bar: 4 μm .) b, c) Backscattered SEM images of the 0.56 wt% AgNW-mixed SBS fibers without AgNPs at pre- and 50% strains. Scale bars: 20 μm . d) Angular distribution of AgNWs aligned along the applied uniaxial strain. Angle θ was evaluated by a reference angle of zero for AgNWs parallel to the uniaxial direction.

stretching. According to the 3D percolation theory, when the concentration of the AgNPs is high enough to satisfy the percolation threshold, the AgNPs in the fibers are connected with each other, forming long-range connectivity and exhibiting the electrical conductivity by the electron hopping.^[31] When the strain is applied to the fiber, the conductivity decreases due to the breakage of the AgNP networks. At a high strain, the fiber will lose its electrical conductivity because the longitudinal distance between AgNPs is too far, as forming cracks between the AgNP networks (left navy-lined box in Figure 3a). On the other hand, when the AgNWs existed in the conductive fiber, the conductivity under high strain can be maintained because the addition of AgNWs will help the networks between AgNPs. We observed the AgNWs located between the cracks of AgNPs (right red-lined box in Figure 3a). In order to examine the effects of the AgNWs on the improved electrical conductivity of the composite fiber under high strain, we observed the backscattered compositional SEM images of the AgNWs inside the composite fiber without AgNPs at pre- and 50% strains (Figure 3b,c). Note that, since the concentration of AgNPs is too high compared to that of the AgNWs, it is hard to recognize the AgNWs from the AgNW–AgNP embedded composite fiber and thus, the AgNW-embedded SBS fibers without AgNPs were used. While the AgNWs inside the SBS fiber were randomly oriented before stretching (Figure 3b), they were aligned along the applied uniaxial strain when the fiber was stretched (Figure 3c). Figure 3d shows the degree of the AgNW alignment under pre- and 50% strains by measuring the deviation angle of the aligned AgNWs with respect to the longitudinal direction of the fiber, indicated by θ in Figure 3b. In the AgNW-mixed SBS fiber, the percentages of AgNWs aligned within $|\theta| \leq 10^\circ$

at the prestrain and 50% strain were 56% and 91%, respectively. Most of the NWs were highly aligned within $|\theta| < 10^\circ$ for the 50% strained fiber. In the mechanical stretching process, 1D structured conductive fillers in a polymer matrix tend to align in the stretching direction due to a torque exerted on the fillers.^[32–34] It is noteworthy that the AgNWs of prestrained fiber were considerably aligned along the longitudinal direction of the fiber (56% within $|\theta| < 10^\circ$). This can be attributed to the fact that when the AgNW-dispersed SBS solutions were extruded from the needle of the syringe pump and coagulated in the PVA liquid for the wet spinning method, the AgNWs in the polymer matrix could be aligned due to the shear and capillary forces.^[35,36] Consequently, we can infer that when the high strain is applied, the well-aligned AgNWs can play important roles inside the composite fiber to connect the broken networks of AgNPs, resulting in an enhancement of the electrical conductivities. Furthermore, we identified some voids between the NWs and the polymer matrix, presumably due to the weak adhesion between the polymer and the NWs.

We constructed a simple circuit consisting of three blue-colored light-emitting diodes (LEDs) connected with 0.56 wt% AgNW reinforced highly stretchable conductive fibers on the bread board to visually confirm the preservation electrical property of the fibers under high strain (Figure S5, Supporting Information). The three LEDs showed stable illumination while the highly stretchable composite fibers were stretched up to 150% strain (Figure 4a). Figure 4b shows the normalized resistance changes ($\Delta R/R_0$) of 0.56 wt% AgNW–AgNP embedded composite fiber under each of the five stretch/release cycles of the applied strains at 20%, 40%, 60%, 80%, and 100%. The response of the normalized resistance of the composite fiber

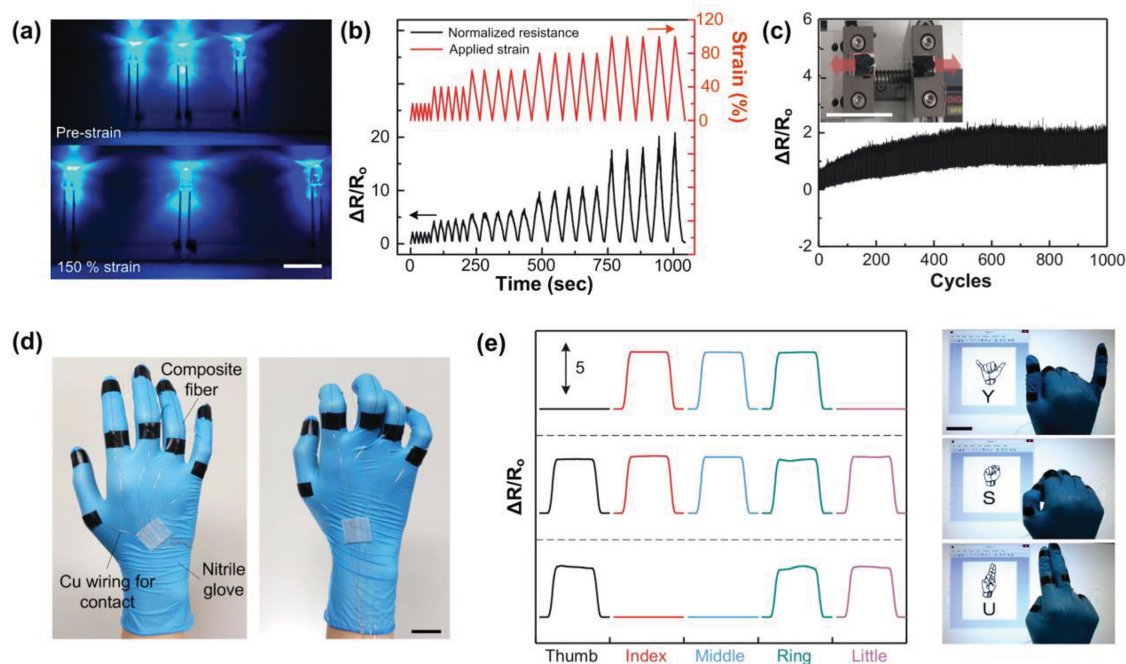


Figure 4. a) Images of blue-colored LEDs connected by 0.56 wt% AgNW–AgNP embedded composite fibers at pre- and 150% strains with 0.1 mA constant current. Scale bar: 1 cm. b) The normalized resistance changes varying the applied strains at 0%, 20%, 40%, 60%, 80%, and 100%. c) Reliability test measured the changes in the normalized resistance of the composite fiber during the stretching and releasing cycle. (The inset shows the photograph of the reliability test with a stretching machine. Scale bar: 3 cm.) d) Photograph of the smart glove attached to the composite fiber on each finger. Scale bar: 2 cm. e) Motion detection of English letters “Y,” “S,” and “U” for utilizing sign language glove and photographs of detecting each letter. Scale bar: 3 cm.

was proportional to the applied strains. The calculated gauge factor, defined as the ratio of the relative change in resistance to the mechanical strain, is ≈ 15 at 100% strain. Compared to the values of previous reports,^[37] the value is quite reasonable for utilizing in the field of the strain gauge. In terms of recovery, it seems that the resistance was fully recovered with a maximum strain of 100%. To precisely evaluate the reliability of our fiber, we observed the long-term reliability test as shown in Figure 4c. This figure represents the normalized resistance profile of the composite fiber by applying 1000 stretch/release cycles from 0% to 10% strains. The inset of Figure 4c shows a photograph of the stretching machine for the reliability test. When the number of cycles is below 600, the peak of the normalized resistance of the composite fiber gradually increases depending on the number of cycles and the baseline also increases. After 600 cycles, the peak and baseline of the normalized resistance did not change. This can be attributed to the structural changes of the AgNW reinforced conductive composite fiber during large mechanical deformation;^[38,39] the AgNPs and aligned AgNWs in the composite fiber were not back to their initial positions after release due to the friction force between conductive fillers and the SBS polymer matrix.^[40] Due to these changed positions of the conductive fillers, certain amount of AgNPs and AgNWs can be physically disconnected with each other. Figure S6 (Supporting Information) shows the surfaces of the composite fibers before and after ten stretch/release cycles from 0% to 100% strain. It was obviously observed that the part of the AgNP network on the surface of the composite fiber was physically broken. Furthermore, there is a possibility

of breaking the AgNWs in the composite fiber as a result of the torque force during repeated stretching and releasing cycles. To identify this effect more precisely, we fabricated a higher concentration of AgNWs (6.75 wt%) containing SBS fiber and measured a backscattered SEM image of AgNWs under a high strain of 100%. As shown in Figure S7 (Supporting Information), the AgNWs were broken into smaller fragments. However, after this phenomenon sufficiently occurred (the number of cycles >600), the peak and baselines of the normalized resistance were stabilized, which means that the composite fiber has a superior electromechanical property with respect to the resistance recovery and long-term reliability at low strain level (10%). We also conducted the reliability test of the composite fiber at high strain, but the fiber did not show reliable property as shown in Figure S8 (Supporting Information). When the reliability test was conducted at 50% strain, the peak and baselines of the normalized resistance were significantly increased and not stabilized. The reason can be explained by the fact that the structural changes and fracture of AgNWs in the composite fiber were severely occurred at high strain and degraded the reliability performance. Furthermore, we conducted a folding test of the composite fiber as shown in Figure S9 (Supporting Information). When the composite fiber was folded, the resistance was 7.8Ω which was similar to that of unfolded composite fiber (7.2Ω). This can be attributed that since the average length of AgNWs was only $20 \mu\text{m}$, the fracture of AgNWs at the folding region in the elastomeric polymer fiber could not significantly affect the degradation of the electrical property of the composite fiber. We also measured the R/R_0 hysteresis curve

of the fiber with the applied strain ranging from 0% to 50% and observed the existence of the hysteresis (Figure S10, Supporting Information). This can originate from the hysteresis of an SBS elastomer.^[41,42]

To demonstrate the utility of the AgNW–AgNP embedded composite fibers in stretchable electronics, we fabricated an artificial glove for detecting sign language the composite fibers that were attached on the glove as a strain gauge sensor to detect the bending motions of the finger joints (Figure 4d). Both ends of each strain sensor adhered to the glove and connected to the circuit for five-channel signal processing by wiring. The circuit receives the measured analog data from the sensors, converts analog signals to the digital signals, and transmits the digital data to a computer. Figure S11 and Movie S1 (Supporting Information) show the motion detection for each finger to confirm the operations of five channels. When the fiber was bent, the resistance corresponding to the strain gauge sensor rapidly increased which means that there is an excellent agreement between the bending fingers and the change in the resistance. Moreover, the sensors exhibited a good response speed, stability, and recoverability. Using this glove, we can detect simple sign language as shown in Figure 4e and Movie S2 (Supporting Information). In order to express the “Y” letter of the English alphabet in sign language, the index, middle, and ring fingers are bent, the changes in the resistance corresponding to the strain sensors were detected from the circuit, and then, the computer recognized and displayed the meaning of the change (Figure 4e). The English letters, “Y,” “S,” and “U,” denoted by Yon-Sei University were successfully detected using the smart glove for sign language. We could easily detect the motion of the human finger by the smart glove integrated with highly stretchable and highly conductive composite fiber.

3. Conclusion

In summary, we have demonstrated AgNW–AgNP embedded highly stretchable conductive fiber using a wet spinning method and an iterative process for Ag precursor absorption and reduction. The initial conductivity of AgNP-embedded SBS fiber without AgNWs increased and became saturated at a three-time treatment of Ag precursor absorption and reduction. The maximum strain at which the conductive fiber was losing its electrical conductivity was 220%, obtained from the 0.56 wt% AgNW and 75 wt% AgNP-embedded composite fiber. The composite fiber also showed preservation of electrical conductivity under high strain. This can be attributed to the fact that the AgNWs were aligned along the uniaxial strain and the aligned AgNWs can act as a bridge between the disconnected networks of AgNPs generated by stretching. Since the fabricated composite fiber has a strain-sensing behavior, we utilized the composite fiber as a strain sensor for detecting human motions. The smart glove was integrated with five composite fibers on each finger and successfully detected simple sign language. We believe that our composite fiber can be applicable to various kinds of stretchable electronics including robotics, e-health care, and wearable smart clothes.

4. Experimental Section

Materials: Ethylene glycol (EG, $\geq 99\%$), AgNO₃ ($\geq 98\%$), DMF (99.5%), THF (99.5%), ethyl alcohol (99.9%), and PVA 500 were purchased from Duksan Pure Chemical. Poly(vinyl pyrrolidone) (PVP, avg $M_w = 55\ 000$), SBS ($M_n = 140\ 000\ \text{g mol}^{-1}$, weight fraction of styrene = 30%), silver trifluoroacetate (AgCF₃COO, 98%), and hydrazine hydrate (N₂H₄·4H₂O, $\approx 50\%–60\%$) were purchased from Sigma-Aldrich.

AgNW Synthesis: For the synthesis of AgNWs, a modified CuCl₂-mediated polyol process was used.^[16,17] 5 mL of EG was prepared in a clean 20 mL vial and heated for 1 h using a silicon oil bath at 151.5 °C with 260 rpm stirring. Then, Cu additive, PVP, and AgNO₃ solutions were added sequentially to the heated EG. 40 μL of a $4 \times 10^{-3}\ \text{M}$ Cu additive solution was injected into the heated EG, and then heated for 15 min. 1.5 mL of a $0.147 \times 10^{-3}\ \text{M}$ PVP solution in EG was then injected into the heated EG. After that, 1.5 mL of a $94 \times 10^{-3}\ \text{M}$ AgNO₃ solution was injected slowly into the mixed solution by a syringe pump at a rate of 0.3 mL min⁻¹ to prevent supersaturation of Ag seeds. Upon nanowire formation after 1 h, the mixed solution was cooled down to room temperature. The synthesized AgNW solution was centrifuged at 2000 rpm and for 30 min with acetone, methanol, and DMF.

Synthesis of Highly Stretchable and Highly Conductive Fibers: The highly stretchable SBS fiber was synthesized by the wet spinning method as shown in the step 1 of Figure 1a. First, SBS was immersed in a solvent mixture of THF/AgNWs-contained DMF (wt/wt = 3:1) for 1 d. The AgNWs were mixed with the SBS solution by stirring for 1 h to form a spinning solution. The spinning solution was injected into a coagulation bath using a syringe pump (NE-300, New Era Pump System, Inc.) with a detachable needle (21 gauge) to control the flow rate of injection. The coagulation bath was filled with 8 wt% of PVA in deionized (DI) water. The wet-spun fibers were collected on the custom-made spool, and dried in air. Then, the wet-spun SBS fiber was dipped in an AgCF₃COO precursor solution (15 wt% in ethanol) as shown in the step 2 of Figure 1b. The fiber was removed from the Ag precursor solution after 30 min and dried at room temperature for 5 min. Hydrazine hydrate (50%) in ethanol was dropped onto the fiber to reduce the absorbed precursor. Since the hydrazine hydrate is very dangerous material, the handling of this material should be very careful. After 5 min, the residual reducing agent was rinsed out several times using DI water and ethanol, and dried on a hot plate for 15 min at 70 °C.

LED and Sign Signal Test: The stretchable conductive fibers were connected with three blue-colored LEDs using silver paste. A simple circuit consisting of two stretchable conductive fibers and three blue-colored LEDs was constructed on the bread board. The illumination of LEDs was observed while the composite fibers were stretched with a constant current (0.1 mA) using a DC source (Keithley 2400 SourceMeter). To test a sign signal, an experimental setup consisting of a resistor divider circuit and voltage measurement tools was prepared. Using the resistor divider circuit, the maximum current applied to the composite fiber was limited to under 50 μA . To obtain the resistance of the fiber, the voltage of the fiber was measured with a constant current using an analog-to-digital converter (ADC) of a microcontroller Atmega128 device. Five composite fibers were attached to each finger one by one and measured via the five-channel ADC. The ADC data were transferred to the computer through serial communication. Then, the movements of the fingers were monitored by the computer, and the motion of the sign signal using the smart glove was determined using the MATLAB program.

Characterization: Surface morphologies were examined using a JEOL JSM-7001F FE-SEM equipped with an EDS system. A stress–strain curve was obtained using a universal testing machine (Korea Polymer Testing & Research Institute). The stretching experiment was carried out using an in-house-built device. The resistance of the fiber was measured as a function of tensile strain by a two-probe method (Fluke, 116 TRUE RMS multimeter). To make the electrical contact to the fiber, a copper tape was attached on a slide glass and then, the fiber was connected to the copper tape/slide glass using a silver paste.

Supporting Information

Supporting Information is available from the Wiley Online Library or from the author.

Acknowledgements

This work was supported by the Priority Research Centers Program (Grant No. 2012-0006689) through the National Research Foundation (NRF) of Korea funded by the Ministry of Education, Science and Technology (MEST) and Mid-career Researcher Program through NRF grant funded by the MEST (Grant No. 2014R1A2A2A09053061). This research was financially supported by the "Sensitivity touch platform development and new industrialization support program" through the Ministry of Trade, Industry&Energy (MOTIE) and Korea Institute for Advancement of Technology (KIAT) (Grant No. R0003423). In addition, the authors would like to acknowledge the support of the Ministry of Higher Education, Kingdom of Saudi Arabia, for supporting this research through a grant (PCSED-009-14) under the Promising Centre for Sensors and Electronic Devices (PCSED) at Najran University, Kingdom of Saudi Arabia. The authors thank Tanaka Kikinzoku Kogyo K.K. for comments on the usage of Ag nanowires and particles.

Received: February 13, 2015

Revised: March 27, 2015

Published online: April 20, 2015

- [1] J. A. Rogers, T. Someya, Y. Huang, *Science* **2010**, 327, 1603.
- [2] T. Sekitani, H. Nakajima, H. Maeda, T. Fukushima, T. Aida, K. Hata, T. Someya, *Nat. Mater.* **2009**, 8, 494.
- [3] L. Hu, M. Pasta, F. L. Mantia, L. Cui, S. Jeong, H. D. Deshazer, J. W. Choi, S. M. Han, Y. Cui, *Nano Lett.* **2010**, 10, 708.
- [4] M. Ramuz, B. C. K. Tee, J. B. H. Tok, Z. Bao, *Adv. Mater.* **2012**, 24, 3223.
- [5] M. Park, J. Im, M. Shin, Y. Min, J. Park, H. Cho, S. Park, M.-B. Shim, S. Jeon, D.-Y. Chung, J. Bae, J. Park, U. Jeong, K. Kim, *Nat. Nanotechnol.* **2012**, 7, 803.
- [6] B. Y. Ahn, E. B. Duoss, M. J. Motala, X. Guo, S.-I. Park, Y. Xiong, J. Yoon, R. G. Nuzzo, J. A. Rogers, J. A. Lewis, *Science* **2009**, 323, 1590.
- [7] J. T. Muth, D. M. Vogt, R. L. Truby, Y. Mengüç, D. B. Kolesky, R. J. Wood, J. A. Lewis, *Adv. Mater.* **2014**, 26, 6307.
- [8] S. Yun, X. Niu, Z. Yu, W. Hu, P. Brochu, Q. Pei, *Adv. Mater.* **2012**, 24, 13217.
- [9] J. Liang, L. Li, K. Tong, Z. Ren, W. Hu, X. Niu, Y. Chen, Q. Pei, *ACS Nano* **2014**, 8, 1590.
- [10] J. Wu, J. Zang, A. R. Rathmell, X. Zhao, B. J. Wiley, *Nano Lett.* **2013**, 13, 2381.
- [11] M. Z. Seyedin, J. M. Razal, P. C. Innis, G. G. Wallace, *Adv. Funct. Mater.* **2014**, 24, 2957.
- [12] A. J. Granero, P. Wagner, K. Wagner, J. M. Razal, G. G. Wallace, M. Panhuis, *Adv. Funct. Mater.* **2011**, 21, 955.
- [13] C. S. Boland, U. Khan, C. Backes, A. O'Neill, J. McCauley, S. Duane, R. Shanker, Y. Liu, I. Jurewicz, A. B. Dalton, J. N. Coleman, *ACS Nano* **2014**, 8, 8819.
- [14] S. Zhu, J.-H. So, R. Mays, S. Desai, W. R. Barnes, B. Pourdeyhimi, M. D. Dickey, *Adv. Funct. Mater.* **2013**, 23, 2308.
- [15] R. Ma, J. Lee, D. Choi, H. Moon, S. Baik, *Nano Lett.* **2014**, 14, 1944.
- [16] K. E. Korte, S. E. Skrabalak, Y. Xia, *J. Mater. Chem.* **2008**, 18, 437.
- [17] J.-Y. Lee, S. T. Connor, Y. Cui, P. Peumans, *Nano Lett.* **2008**, 8, 689.
- [18] C. M. Hansen, *Ind. Eng. Chem. Prod. Res. Dev.* **1969**, 8, 2.
- [19] J. Brandrup, E. H. Immergut, E. A. Grulke, A. Abe, D. R. Bloch, *Polymer Handbook*, 4th ed., Wiley, Chichester, UK **2005**.
- [20] J. Choi, S. Y. Kwak, S. Kang, S. S. Lee, M. Park, S. Lim, J. Kim, C. R. Choe, S. I. Hong, *J. Polym. Sci., Part A: Polym. Chem.* **2002**, 40, 4368.
- [21] E. Díez, G. Ovejero, M. D. Romero, I. Díaz, S. Bertholdy, *Chem. Eng. Trans.* **2011**, 24, 553.
- [22] Y.-X. Wang, C.-G. Wang, M.-J. Yu, *J. Appl. Polym. Sci.* **2007**, 104, 3723.
- [23] P. Sobhanipour, R. Cheraghi, A. A. Volinsky, *Thermochim. Acta* **2011**, 518, 101.
- [24] S. E. Morris, Y. Bayram, L. Zhang, Z. Wang, M. Shtein, J. L. Volakis, *IEEE Trans. Antennas Propag.* **2011**, 59, 3458.
- [25] B. K. Little, Y. Li, V. Cammarata, R. Broughton, G. Mills, *ACS Appl. Mater. Interfaces* **2011**, 3, 1965.
- [26] F. Ochanda, W. E. Jones, Jr., *Langmuir* **2005**, 21, 10791.
- [27] C. Han, M. Bai, J. Lee, *Chem. Mater.* **2001**, 13, 4260.
- [28] D. Stauffer, *Introduction to Percolation Theory*, Taylor and Francis, London **1992**.
- [29] J. Li, J.-K. Kim, *Compos. Sci. Technol.* **2007**, 67, 2114.
- [30] B. Lin, G. A. Gelves, J. A. Haber, U. Sundararaj, *Ind. Eng. Chem. Res.* **2007**, 46, 2481.
- [31] Z. J. Han, B. K. Tay, *J. Appl. Polym. Sci.* **2008**, 107, 3332.
- [32] Q. Wang, J. Dai, W. Li, Z. Wei, J. Jiang, *Compos. Sci. Technol.* **2008**, 68, 1644.
- [33] L. Jin, C. Bower, O. Zhou, *Appl. Phys. Lett.* **1998**, 73, 1197.
- [34] Q. Liu, M. Li, Y. Gu, Y. Zhang, S. Wang, Q. Li, Z. Zhang, *Nanoscale* **2014**, 6, 4338.
- [35] A. J. Ryan, *Polymer Processing and Structure Development*, Kluwer, Dordrecht, The Netherlands **1998**.
- [36] H. Lee, B. Seong, J. Kim, Y. Jang, D. Byun, *Small* **2014**, 10, 3918.
- [37] M. Amjadi, A. Pichitpajongkit, S. Lee, S. Ryu, I. Park, *ACS Nano* **2014**, 8, 5154.
- [38] M. Vural, A. M. Behrens, O. B. Ayyub, J. J. Ayoub, P. Kofinas, *ACS Nano* **2015**, 9, 336.
- [39] W. Hu, X. Niu, L. Li, S. Yun, Z. Yu, Q. Pei, *Nanotechnology* **2012**, 23, 344002.
- [40] F. Xu, Y. Zhu, *Adv. Mater.* **2012**, 24, 5117.
- [41] M. Ashida, W. Guo, *J. Appl. Polym. Sci.* **1993**, 49, 573.
- [42] G. R. Hamed, *J. Adhes.* **1983**, 16, 31.